PNAS

# Supporting Information for

Cytoskeleton remodeling mediated by circRNA-YBX1 phase separation suppresses the metastasis of liver cancer.

Boqiang Liu[1,2,3,4,†], Hao Shen[1,2,3,4,†], Jing He[1,2,3,4], Binghan Jin[5], Yuanshi Tian[6], Weiqi Li[1,2,3,4], Lidan Hou[1,2,3,4], Weijun Zhao[1,2,3,4], Junjie Nan[1,2,3,4], Jia Zhao[2], Jiliang Shen[1,2,3,4], Hong Yu[1,2,3,4], Yifan Wang[1,2,3,4], Ge Shan[7, 8, 9], Liang Shi[1,2,3,4,*] and Xiujun Cai[1, 2, 3, 4, 7, *]

Liang Shi
Email: Liang_Shi@zju.edu.cn
Xiujun Cai
Email: srrsh_cxj@zju.edu.cn

**This PDF file includes:**

## Methods

### Patient Samples

A total of 3 independent cohorts including 145 HCC patients were used in this study. Cohort 1 contained a small group of 22 randomly selected HCC clinical samples collected from Sir Run-Run Shaw Hospital starting in August 2018, which were used for detecting the expression levels of circASH2, mASH2, and DHX9. Cohort 2 included 11 highly and 21 low invasive primary HCC samples collected from Sir Run-Run Shaw Hospital starting in January 2018, which were used for screening metastasis-related circRNAs. Cohort 3 included 91 randomly selected HCC clinical samples with follow-up information, which were collected from Sir Run-Run Shaw Hospital starting in February 2006. Patients in cohort 3 were monitored with a 5-y follow-up. The follow-up period was defined as the interval from the date of surgery to the date of recurrence or death. Patients alive at the end of follow-up were censused. DFS was defined as the interval from the date of surgery until the detection of tumor recurrence. Patients without signs of recurrence at the end of follow-up were censused. Patients who died from diseases other than HCC or unexpected events were excluded from the study cohort. The low and high circASH2 expressions were cut off by median expression.

This study conformed to the principles of the Declaration of Helsinki and was approved by the Ethics Committee of Sir Run-Run Shaw Hospital (SRRSHLS2022Y0312). All patients signed informed consent before surgery for the use of their tissues for scientific research.

### Animals.

Male 8-wk-old BALB/C nude mice were used for experiments. HA22T cells were engineered to express the luciferase reporter gene by stable transfection, and the positive stable clones were selected with ampicillin and expanded in culture(1). After that, stable overexpressing circASH2 or control vector HA22T cells were established.

For the orthotopic xenograft model, these cells were injected into nude mice orthotopically to generate and maintain HA22T HCC tissues. The orthotopic models were prepared by transplanting these HCC tissues into mice's liver by a surgical approach. Briefly, two groups of 14 mice each were planted with 1 mg HA22T HCC tissues (HA22T-circASH2 or HA22T-vector) into the left lobe of the liver. Tumor formation and metastasis were monitored by using a Fluorescent Imager [IVIS (In vivo image system) Spectrum] starting from the third day after tumor injection and using mouse intraperitoneal injection of 150 mg/kg D-Luciferin solution. Mice injected with HCC cells were killed after 12 wk, and samples were isolated for further testing. For the tail vein injection model of metastasis, mice (n = 8) were injected with control or oe-circASH2 cells (1 × 106 cells/mouse) through the tail vein. Metastasis was tracked by the IVIS system mentioned before once every 2 wk thereafter. For the intrasplenic injection model of metastasis, engineered cells (1 × 106 cells/mouse) were injected into the mouse spleen (n = 6), and liver metastases were examined in the 9th week after the injection.

### Cell culture

LO2, HCCLM3, HA22T, Hep-SK1 were maintained in DMEM (Invitrogen) with 10% fetal bovine serum (FBS, Cellmax), and 1% Glutamine. Huh7 cell was maintained in MEM (Invitrogen) with 10% FBS, and 1% Glutamine. All cells were cultured at 37 °C and 5% CO2. And all cells were checked for mycoplasma by a PCR-based method as well as DAPI staining, to ensure the absence of contamination. Cell line sources are described in supplementary file.

### Human circRNA microarray

The Human circRNAs chip (ArrayStar), containing more than 40000 probes specific for human circRNAs splicing sites, was used. After hybridization and washing with samples, 10 primary HCC tissues were analyzed on the circRNAs chips. Exogenous RNAs developed by the External RNA Controls Consortium were used as controls. The sequencing and analysis procedures were performed by Aksomics Co., Ltd.

### Lentiviral infection and siRNA transfection

Cells with stable expression were established based on a previous report(1). Briefly, HEK293 cells were transfected with the 20 ug core plasmid (LentiCRSPRv2, pLVX, pLO5-ciR, or pLC5-ciR), with 10 ug psPAX2 packaging plasmid, and 10ug pMD2.G envelope plasmid, for 48 hours to obtain the lentivirus supernatant, which was frozen at -80°C for later infection (1mL lentivirus supernatant /1 $\times 10^6$ HCC cells for 8 hour) to produce stable polyclonal populations. Among them, pLO5-ciR (without GFP sequence) and pLC5-ciR (with GFP sequence) core plasmids are specialized circRNA over-expression vectors, containing circRNA over-expression framework (such as Alu element, QKI and other RBP binding sites), and could ensure accurate and efficient circRNA cyclization through unique cyclization mediated sequences. EcoRI and BamHI cleavage sites were reserved in the middle of the expression framework, which could be directly inserted with the target circRNA sequence.

For siRNA transfection, we used LipofectAMINE 3000 (Invitrogen), according to the manufacturer's instructions. Briefly, in order to successfully knock-down target, 0.2 nmol specific siRNA and 10 uL LipofectAMINE 3000 are needed and should be mixed well. The final concentration of siRNA in the transfection system is 100 nM. 8 hours after transfection, the culture-medium should be changed, And, the knock-down efficiency could be detected 48 hours later. Also, sgRNAs for CRISPR were generated by following LentiCRSPRv2 manufacturer's instructions (2).

**Quantitative real-time PCR**

Total RNAs were isolated using Trizol reagent (Invitrogen), either from cultured cells or frozen tissue of primary tumors and adjacent non-tumor liver tissues. One microgram of total RNA was subjected to reverse transcription using Superscript III transcriptase (Invitrogen). Quantitative real-time PCR (RT-qPCR) was conducted using a Bio-Rad CFX96 system (Bio-Rad) with SYBR green to determine the expression level of a targets of interest. Expression levels were normalized to the expression of GAPDH mRNA. The detecting primers for circRNAs were designed based on its head-to-tail junction(1).

**Cell adhesion, migration and invasion assays**

For trypsin digestion assay, same amount of HCC cells was seeded for overnight. Then commercial trypsin with EDTA was used for 0.5-2 minutes digestion. Digested cells were washed, and remaining cells were fixed by 4% paraformaldehyde and stained by 0.1% crystal violet for observation.

For 3D invasion assay, we first generated HA22T spheroids (vector or oe-circASH2, diameter= 50 um) in Nunclon Sphera 96U-well plate (Invitrogen) according to the manufacturer's instructions. Then, we transferred the HA22T spheroids to a medium containing matrix, and observed the invasion of spheroids in the matrix one week later.

For transwell assay, HCC cells were seeded with serum-free medium into the upper chamber at 0.2-1×$10^5$ cells/well, and the bottom chamber of the apparatus contained culture medium with 10% FBS, and then incubated for 24 hours at 37°C. Following incubation, the migrated cells attached to the lower surface of the membrane were fixed by 4% paraformaldehyde and stained with 0.1% crystal violet for observation. To acquire the dynamic metastasis curve, the real-time xCELLigence cell analyser RTCA (Roche Diagnostics) was used to measure cell migration over time for 48 hours.

**Next generation sequencing**

Total RNA was extracted by using Trizol reagent (Invitrogen) according to the manufacturer's instructions. The concentration and quality of total RNA were measured by Nanodrop and verified by gel electrophoresis. Then, the total RNA was sent to TSINGKE Biological Technology Co., Ltd. for library construction, sequencing and analysis.

**Cell lysis, immunoprecipitation (IP) and immunoblotting (IB)**

Cells were homogenized in RIPA or IP lysis buffer supplemented with Protease Inhibitor Cocktail, Phosphatase Inhibitor Cocktail, Panobinostat, and Methylstat. Lysates were cleared by centrifugation at 13,000 rpm for 15 minutes at 4°C. Supernatants were analyzed for immunoblotting or for immunoprecipitation with the indicated antibodies. For immunoprecipitation,

the prepared cell lysates were precleared using 10 μL Protein A+G Agarose beads by rotating at 4°C for 3 hours. Add the indicated antibody and control IgG to the precleared lysates followed by adding 20 μL Protein A+G Agarose beads to the mixture with rotating the tubes at 4°C for 3-5 hours for each process. The protein-captured beads were washed with lysis buffer three times and eluted with 50 μL SDS loading buffer and the eluted protein or protein complexes were detected by immunoblot. Proteins were separated on 10-15% SDS/PAGE gel and then transferred onto PVDF membranes (Millipore). After blocking, membranes were incubated with appropriate dilutions of specific primary antibodies followed by incubation with HRP-conjugated secondary antibodies and visualization using ECL system (Bio-Rad).

**RNA FISH assay and immunofluorescence (IF) staining**

RNA Fluorescence in situ hybridization (FISH) was performed with a FISH kit (Ribobio) according to the manufacturer's instruction. Briefly, cells in chamber slides were fixed in 4% formaldehyde for 15 minutes. The air-dried cells were subjected to incubation with 40 nM Cy3-conjugated FISH probe (Ribobio) in hybridization buffer (100 mg/ml dextran sulfate, 10% formamide in 2xSSC) at 80°C for 2 minutes. The hybridization was performed at 55°C for 2 hours and the slide was washed with 0.1xSSC at 65°C followed by dehydration through 70%, 90% and 100% ethanol. Next the slides were used for further IF staining or, mounted with Prolong Gold Antifade Reagent with DAPI for confocal microscopy detection.

For immunofluorescence, cells were cultured in chamber slides overnight and fixed with 4% formaldehyde in PBS for 10 minutes at 4°C, followed by permeabilization with 0.5% Triton X-100 in PBS for 10 minutes. Cells were then blocked for nonspecific binding with 10% goat serum in PBS and 0.1% Tween-20 (PBST) overnight, and incubated with the indicated antibody for 1 hour at room temperature, followed by incubation with Goat anti-Mouse or anti-Rabbit IgG (H+L) Antibody from Abcam for 1 hour at room temperature. For stress fiber staining, Rhodamine Phalloidin F-actin Stain Kit from Invitrogen was used. Coverslips were mounted on slides using anti-fade mounting medium with DAPI. Immunofluorescence images were acquired on an Olympus FV3000 fluorescence microscope. For each channel, all images were acquired with the same settings.

**Luciferase reporter assay**

Luciferase reporter assay was performed according to the standard protocol of Dual-Luciferase Reporter Assay system (Promega). Briefly, indicated fragments of TPM4 promoter (-2000-0 bp) was cloned into the pGL3 luciferase reporter vector, and transfected into circASH2-silenced and control HCC cells (Huh7 and HCCLM3). For each sample, 1 ng pRL-TK was transfected as loading control. 48 hours later, cells were collected and lysed by lysis buffer followed by detection of luciferase activity.

**RNA pulldown and purification**

For circRNA pulldown assays, cells lysates were prepared by using IP lysis buffer and followed the manufacturer's instruction of Pierce Magnetic RNA-Protein Pull-Down Kit (Thermo Fish Scientific). Briefly, washed Pierce Streptavidin Magnetic Beads were incubated with cell lysate at 4°C for 1 hour for preclearance. The 3' biotin-labeled circRNA probe incubated with the beads at RT for 10 minutes for immobilization. Then, the biotinylated beads were incubated with cell lysate at 4°C overnight. The biotinylated beads were magnetically separated and washed five times. For western blot detection, the beads were boiled in SDS buffer for protein/peptide isolation. For mass spectrometry assays, the beads were incubated with non-ionic water in 70°C for 5 minutes. For RT-qPCR assays and circRNA purification, Trizol reagent was used to extract the total RNA from the beads.

**Mass spectrometry analysis**

The peptide samples collected from Huh7 and HCCLM3 cells were analyzed on Q-Extractive mass spectrometer (Thermo Fish Scientific) by Novegene Co., Ltd. The full mass and subsequent MS/MS analyses were performed in an Orbitrap analyzer with a resolution of 70000 for MS1 (at 200 mass/charge ratio [m/z]) and 17500 for MS2, respectively. The automatic gain control target for MS1 was set to $3.0\times10^{+6}$ with max inject time (IT) of 50ms and $5.0\times10^{+4}$ for MS2 with max IT

100ms. The top 20 most intense ions were fragmented by HCD with normalized collision energy of 27% and isolation window of 2 m/z. The dynamic exclusion was set at 30 seconds. Raw data were processed with MaxQuant software (version 1.5.6.0). The intracellular pathway analysis was performed using clusterProfiler in R package to search Gene Ontology (GO) and Kyoto Encyclopedia of Genes and Genomes (KEGG) database.

**RNA immunoprecipitation (RIP) and RNA extraction**

To prepare antibody-coated beads, 20 μL Protein A+G Agarose beads were incubated with 1-5 mg antibody or control IgG in 500 μL lysis buffer supplemented with Protease Inhibitor Cocktail, Phosphatase Inhibitor Cocktail Panobinostat and Methylstat at 4°C overnight. Then, the beads were washed twice with lysis buffer and kept on ice. Cell lysates were precleared using 10uL Protein A+G Agarose beads by rotating at 4°C for 3 hours. The precleared lysates were transferred to tubes with antibody-coated beads, and then rotated tubes at 4°C for 3-5 hours. The protein-captured beads were washed with lysis buffer for three times. RNA extraction from the beads was collected by using Trizol according to the manufacturer's instructions for later detection. Also, nuclear and cytoplasmic RNA isolation were by using PARIS™ Kit (Thermo Fish Scientific) according to manufacturer's instruction.

**circRNA/mRNA interaction simulation and analysis**

In the secondary structures of circRNA, the first and last base forms the junction site(3). To determine the secondary structures with minimum free energy, we used Mfold (version2.3, http://unafold.rna.albany.edu/?q=mfold) to calculate(4). Mfold uses energy minimization to identify optimal folding of a nucleic-acid sequence within a specified energy increment in order to simulate the ensemble of possible structures. According to Mfold's calculation, the best secondary structure for circASH2 would have a free energy of -162.70 kcal/mol. And the secondary structure with lowest theoretical value of free energy would be chosen for 3D modeling.

Dot-Bracket Notation was the filed used for RNA Composer (http://rnacomposer.cs.put.poznan.pl/) to generate the 3D model(5). RNA Composer is a web-based software for RNA folding and 3D structure prediction. Then we used RNA Composer to analyze the tertiary structure and generated the 3D model of circASH2.

RNA loops are known to be the key structure to mediate the RNA interactome(6). We mutated all hairpin structures with bases greater than 8 separately. The principle of mutation we adopted is randomly mutate A/T base to G/C base and vice versa. The corresponding mRNA sequences were obtained by BLAST (https://blast.ncbi.nlm.nih.gov/Blast.cgi).

**circRNA/protein interaction simulation and analysis**

The 3D model of circASH2 was put in HDOCK software (http://hdock.phys.hust.edu.cn/) together with YBX1 (PDB No. 1H95) for RNA/Protein interaction simulation(7). Distance-based approach was used to identify the binding site residues/nucleotides for the protein-RNA complexes using a specific cutoff value. Two atoms (one in RNA and another in protein) were considered to be interacting with each other if the distance between them was <4.5Å.

Bases that might be responsible for interaction was also acquired from HDOCK, according to the distance to YBX1. Then, we generated mutations in circASH2 for binding to YBX1, namely circASH2$^{YBX1mut}$. The principle of mutation is as same as above. Since the mutation sites were not completely continuous, we re-composed the whole 580 bases of circASH2 according to mutation blueprint. After reconstructing the plasmid, we verified the ring formation and mutation by specifically designed primers and sequencing.

**Chemical treatment and inhibitor incubation assays**

All the chemicals and inhibitors were prepared as manufacturer suggested. Actinmyocin D was used in RNA decay tests at a concentration of 2 ug/ml. Pre-mRNA splicing inhibitors Madrasin, Isoginkgetin and Hinokiflavone were used to interfere pre-mRNA splicing at the concentration of 10-20 uM, 5-10 uM, 5-10 uM, respectively. NMD inhibitors eIF4A3-IN-1 and NMDI14 treated cells at the same concentration of 5-10 uM. 5% (v/w %) PEG8000 was used as crowded reagent in LLPS assays, and 5% (v/w %) 1,6-hexanediol was used to disassemble YBX1 puncta.

**Phase separation assay in cells**

HCC cells (Huh7, HCCLM3 and HA22T) expressing YBX1-GFP were grown on coverslips. After adhering to coverslips, cells were analyzed by Olympus FV3000 confocal microscopy, and the visible puncta with diameter more than 0.5 μm were defined as LATS1 puncta.

***In vitro* phase separation assay**

*In vitro* phase separation assay was performed in storage buffer with indicated protein concentrations, and PEG8000 was also added to a final concentration of 10% (w/v). Phase separation assay was carried out on glass-bottomed dishes, sealed with optically clear adhesive film to prevent evaporation and observed under an Olympus FV3000 confocal microscope equipped with 60× oil immersion objectives. The phase separation assay using circASH2 and YBX1-GFP was performed in a physiological LLPS buffer (20 mM Tris-HCl, pH 7.5, 15 mM NaCl, 130 mM KCl, 5 mM $KH_2PO_4$, 1.5 mM $MgCl_2$, and 1 mg/mL BSA).

**FRAP assays**

FRAP experiments were performed on an Olympus FV3000 confocal microscope with a 60× oil immersion objective. For the *in vitro* experiments, droplets were photobleached with 50% laser power for 0.5 seconds using 488-nm lasers. Time-series images were acquired every ten seconds after bleaching for 5 minutes. For the *in vivo* experiments, FRAP assays were carried out on an OLYMPUS FV3000 confocal microscope at 37 °C in a live-cell-imaging chamber. The recovery from photobleaching was recorded for the indicated time. Analysis of the recovery curves was carried out with ImageJ software.

**Quantification and statistical analysis**

The experiment was set up to use at least 3 samples (biological replicates) per experiment/ group/ condition to detect a 2-fold difference with power of 80% and at the significance level of 0.05 by a two-sided test for significant studies. Results are reported as mean ± Standard Deviation (SD). Comparisons were performed using two-tailed paired Student's t test, one-way ANOVA test or two-way ANOVA test, as indicated in individual figures. For survival analysis, the expression of indicated targets was treated as a binary variant and divided into 'high' and 'low' level. Kaplan-Meier survival curves were compared using the Gehan-Breslow test in GraphPad Prism v6.01.

**Materials**

**Antibodies**

| Name | Supplier | Cat No. |
|---|---|---|
| Rabbit anti-TPM4 antibody [EPR13316] | Abcam | Cat# ab181085 |
| Rabbit anti-DHX9 antibody [EPR13521] | Abcam | Cat# ab183731 |
| Rabbit anti-ADAR1 antibody [EPR7033] | Abcam | Cat# ab126745 |
| Rabbit anti-QKI antibody [EPR7306] | Abcam | Cat# ab126742 |
| Mouse anti-E Cadherin antibody [rCDH1/1525] | Abcam | Cat# ab238099 |
| Rabbit anti-N Cadherin antibody [EPR1791-4] | Abcam | Cat# ab76011 |
| Rabbit anti-Vimentin antibody [EPR3776] | Abcam | Cat# ab92647 |
| Rabbit anti-YBX1 antibody [EP2708Y] | Abcam | Cat# ab76149 |
| Rabbit anti-Paxillin antibody [Y113] | Abcam | Cat# ab32084 |
| Rabbit anti-UPF1 antibody [EP4682] | Abcam | Cat# ab133564 |
| Rabbit anti-hnRNPA1 antibody [9H10] | Abcam | Cat# ab5832 |
| Rabbit anti-hnRNPD antibody [EPR24001-12] | Abcam | Cat# ab259895 |
| Rabbit anti-hnRNPK antibody [3C2] | Abcam | Cat# ab39975 |
| Rabbit anti-N6-methyladenosine antibody [17-3-4-1] | Abcam | Cat# ab208577 |
| Mouse anti-DDDDK tag (Binds to FLAG® tag sequence) antibody [M2] (HRP) | Abcam | Cat# ab49763 |
| Rabbit anti-6X His tag antibody [EPR20547] | Abcam | Cat# ab213204 |
| Rabbit anti-GFP antibody [EPR14104] | Abcam | Cat# ab183734 |
| Rabbit IgG, monoclonal [EPR25A] - Isotype Control | Abcam | Cat# 172730 |
| Mouse IgG, monoclonal - Isotype Control | Abcam | Cat# 37355 |
| Rabbit anti-TPM4 antibody (ICC) | Invitrogen | Cat# 720311 |
| Goat anti-Rabbit IgG (H+L) Antibody, Alexa Fluor 488 | Invitrogen | Cat# A32731 |
| Rabbit anti-Phospho-FAK (Tyr397) antibody (D20B1) | Cell Signaling Technology | Cat# 8556 |
| Rabbit anti-FAK antibody (D2R2E) | Cell Signaling Technology | Cat# 13009 |
| Rabbit anti-Akt (pan) (11E7) Rabbit mAb | Cell Signaling Technology | Cat# 4685 |
| Rabbit anti-Phospho-Akt (Ser473) (D9E) Rabbit mAb | Cell Signaling Technology | Cat# 4060 |
| Rabbit anti-PI3 Kinase p85 (19H8) Rabbit mAb | Cell Signaling Technology | Cat# 4257 |
| Rabbit anti-Phospho-PI3 Kinase p85 (Tyr458)/p55(Tyr199) (E3U1H) Rabbit mAb | Cell Signaling Technology | Cat# 17366 |
| Rabbit anti-GAPDH antibody (D4C6R) | Cell Signaling Technology | Cat# 97166 |
| Rabbit anti-Histone H3 antibody (D1H2) | Cell Signaling Technology | Cat# 4499 |
| ANTI-FLAG® M2 Affinity Gel | Sigma-Aldrich | Cat# A2200 |

**Cell lines**

| Name | Supplier | Cat No. |
|---|---|---|
| Human: LO2 | Institute for Advanced Study of Central South University | Cat# HTCC01 |
| Human: Huh7 | JCRB | Cat# JCRB0403 |
| Human: HCCLM3 | Type Culture Collection of Chinese Academy of Science | Cat# SCSP-528 |
| Human: HA22T | BCRC | Cat# 60168 |
| Human: SK-Hep1 | ATCC | Cat# HTB-52 |
| Human: Hep-G2 | ATCC | Cat# HB-8065 |
| Human: HEK293 | ATCC | Cat# CRL-1573 |

**Primer and oligo sequences**

| Name | Sequence | Supplier |
|---|---|---|
| circASH2 biotinylated probe | aaaTAAATGGTATAATATCCTCGATCATGTAGGG | TsingKe |
| circASH2 antisense biotinylated probe | aaaATTTACCATATTATAGGAGCTAGTACATCCC | TsingKe |
| circPABPC1 biotinylated probe | aaaCAGCACGGTTCTGAGTGATGAGGTCTGGCAC | TsingKe |
| circASH2 probe with Cy3 conjugated | aaaTAAATGGTATAATATCCTCGATCATGTAGGG | Ribobio |
| TPM4 pre/mRNA probe (mix) with Cy5 conjugated | AGCCCTG+TCCAACTCCTCCTCAACGA TCCGCACGCTCC+TCTGCCCTCT GCTACC+TCCTCGTAT+TTGCGGTCAG | Gene Pharma |
| si-circASH2 | GATCGAGGATATTATACCA | Ribobio |
| si-mASH2L | CAGTAAAGATCCAGAAGAA | Ribobio |
| si-DHX9-1 | CGAACACCATTGCATGAAA | Ribobio |
| si-DHX9-2 | GGACTAGTAGCAACATTGA | Ribobio |
| si-ADAR1-1 | GCAGAGTCAGCATATATGA | Ribobio |
| si-ADAR1-2 | GGCCCGAGATATAAATGCT | Ribobio |
| si-QKI-1 | GAAGCTGGTTTAATCTATA | Ribobio |
| si-QKI-2 | GACCTATTGTTCAGTTACA | Ribobio |
| ASO-circASH2 | CCCTACATGATCGAGGATAT | Ribobio |
| sgRNA-YBX1 | CAGTAAAATGGTTCAATGTA | TsingKe |
| sgRNA-TPM4 | CGAGCTGGATAAATATTCCG | TsingKe |
| sgRNA-UPF1 | GGTAGGCGTCCTCGTACCGC | TsingKe |
| circASH2 qPCR primer (except circASH2-random2) -F | CAAGCGCAAACAGCAGGATG | TsingKe |
| circASH2 qPCR primer (except circASH2-random2) -R | TTCCCACTAGTAGACACAGCA | TsingKe |
| circASH2 qPCR primer (for circASH2-random2)-F | TGGAACTTGACTGCTGGGC | TsingKe |
| circASH2 qPCR primer (for circASH2-random2)-R | TAATATCCTCGATCATGTAGGGCT | TsingKe |
| ASH2L qPCR primer-F | TTTGTTTTCTGCTCAGCGCC | TsingKe |

| | | |
|---|---|---|
| ASH2L qPCR primer-R | TCAAGTTCCAGCTTCTCGGG | TsingKe |
| GAPDH qPCR primer-F | CGACCACTTTGTCAAGCTCA | TsingKe |
| GAPDH qPCR primer-R | TTACTCCTTGGAGGCCATGT | TsingKe |
| pre-GAPDH qPCR primer-F | TGGGGACTGGCTTTCCCATAA | TsingKe |
| pre-GAPDH qPCR primer-R | GCCAGTAGAGGCAGGGATGA | TsingKe |
| β -actin qPCR primer-F | CATGTACGTTGCTATCCAGGC | TsingKe |
| β -actin qPCR primer-R | CTCCTTAATGTCACGCACGAT | TsingKe |
| pre- β -actin qPCR primer-F | TGTGTGGGGAGCTGTCACAT | TsingKe |
| pre- β -actin qPCR primer-R | TCCGCCTAGAAGCATTTGCG | TsingKe |
| DHX9 qPCR primer-F | CGAACCATCTCAGCGACAAAA | TsingKe |
| DHX9 qPCR primer-R | TGAGGTCCATGCTTATTTGCTC | TsingKe |
| ADAR1 qPCR primer-F | CTGAGACCAAAAGAAACGCAGA | TsingKe |
| ADAR1 qPCR primer-R | GCCATTGTAATGAACAGGTGGTT | TsingKe |
| QKI qPCR primer-F | AAGCCCACCCCAGATTACCT | TsingKe |
| QKI qPCR primer-R | ACTCTGCTAATTTCTTCGTCCAG | TsingKe |
| TPM4 qPCR primer (except TPM4-ΔCDS)-F | GAGGTAGCTCGTAAGCTGGTC | TsingKe |
| TPM4 qPCR primer (except TPM4-ΔCDS)-R | ACCGTTCTCTCTGCAAATTCAG | TsingKe |
| TPM4 qPCR primer (for TPM4-ΔCDS)-F | TCGGAGAAGCTTTGAGCACC | TsingKe |
| TPM4 qPCR primer (for TPM4-ΔCDS)-R | TGTGATGGTCCCTGGTCTCT | TsingKe |
| pre-TPM4 qPCR primer-F | CTGATGCTTTGGCGGAGGAA | TsingKe |
| pre-TPM4 qPCR primer-R | TCACGAACGTTCTCACTCTCC | TsingKe |
| ZNF616 qPCR primer-F | CAGTGACCGTTCAGCTTTTGC | TsingKe |
| ZNF616 qPCR primer-R | CGATGCCCTACAAGATGTGAAT | TsingKe |
| PPL qPCR primer-F | CCGGAGCATCTCTAACAAGGA | TsingKe |
| PPL qPCR primer-R | GCATCCGCCTCTAGCACAT | TsingKe |
| MPZ qPCR primer-F | CATCGTGGTTTACACCGACAG | TsingKe |
| MPZ qPCR primer-R | TGGAAGATCGAAATGGCATCTCT | TsingKe |
| MICB qPCR primer-F | TCTTCGTTACAACCTCATGGTG | TsingKe |
| MICB qPCR primer-R | TCCCAGGTCTTAGCTCCCAG | TsingKe |
| MAN2A1 qPCR primer-F | CAGTGCGATCTTCTGTGTGGT | TsingKe |
| MAN2A1 qPCR primer-R | GCAAACGCTCCAAATGGTCTAT | TsingKe |
| LRRC58 qPCR primer-F | ACTTGCTGACATATCTGCCTCG | TsingKe |
| LRRC58 qPCR primer-R | CAGGAGAGTTGGAGGATCATAGG | TsingKe |
| GNG12 qPCR primer-F | GCAAAACAGCAAGCACCAAC | TsingKe |
| GNG12 qPCR primer-R | CTATCAGCAAAGGGTCACTCC | TsingKe |
| GAL3ST1 qPCR primer-F | ACCACATGCGCTTCCACTAC | TsingKe |
| GAL3ST1 qPCR primer-R | GGTCTTGCAGGAACTCGGT | TsingKe |
| EIF2A qPCR primer-F | CCGCTCTTGACAGTCCGAG | TsingKe |
| EIF2A qPCR primer-R | GCAGTAGTCCCTTGTTAGTGACA | TsingKe |
| CRYAB qPCR primer-F | CCTGAGTCCCTTCTACCTTCG | TsingKe |
| CRYAB qPCR primer-R | CACATCTCCCAACACCTTAACTT | TsingKe |
| CCND1 qPCR primer-F | GCTGCGAAGTGGAAACCATC | TsingKe |

| | | |
|---|---|---|
| CCND1 qPCR primer-R | CCTCCTTCTGCACACATTTGAA | TsingKe |
| UPF1 qPCR primer-F | ACCGACTTTACTCTTCCTAGCC | TsingKe |
| UPF1 qPCR primer-R | AGGTCCTTCGTGTAATAGGTGTC | TsingKe |

**Biological samples**

| Description | Source |
|---|---|
| Human HCC tumor tissue and paired liver tissue | Sir Run Run Shaw Hospital, Zhejiang University |

**Compounds, proteins, vectors etc.**

| Description | Source | Identifier |
|---|---|---|
| WB/IP lysis buffer | Beyotime | Cat# P0013J |
| Anti-fluorescence quenching mounting solution | Beyotime | Cat# P0128M |
| Protein A+G Agarose | Beyotime | Cat# P2055 |
| TRIzol | TAKARA | Cat# 15596026 |
| Polybrene | Sigma-Aldrich | Cat# H9268 |
| DNA Marker DL2000 | Vazyme | Cat# MD101-01 |
| Protease inhibitor cocktail | Abcam | Cat# ab65621 |
| Phosphatase inhibitor | Invitrogen | Cat# 78442 |
| Invitrogen™ ProLong™ gold antifade mountant with DAPI | Invitrogen | Cat# P36935 |
| HEPES (1 M) | Invitrogen | Cat# 15630080 |
| Lipofectamine 3000 reagent | Invitrogen | Cat# L3000015 |
| Tyrpsin-EDTA (0.5%) | Invitrogen | Cat# 15400054 |
| Yeast tRNA (10 mg/mL) | Invitrogen | Cat# AM7119 |
| Yeast RNA (5 mg/mL) | Invitrogen | Cat# AM7120G |
| Streptavidin magnetic beads | Invitrogen | Cat# 88817 |
| RNase A | Invitrogen | Cat# EN0531 |
| Rnase R | Epicentral | Cat# RNR07250 |
| Ultrapure Salmon Sperm DNA | Invitrogen | Cat# 15632011 |
| RNase Inhibitor, recombinant (human placenta) | New England Biolabs | Cat# M0307S |
| Matrigel Basement Membrane Matrix | BD biosciences | Cat# 356237 |
| D-Luciferin, Sodium Salt D | Yeasen Biotech | Cat# 40901ES01 |
| 1,6-hexanediol | Sigma-Aldrich | Cat# 240117 |
| PEG 8000 | Sigma-Aldrich | Cat# 89510 |
| Actinomycin D | Cell Signaling Technology | Cat# 15021 |
| Madrasin | MedChemExpress | Cat# HY-100236 |
| Isoginkgetin | MedChemExpress | Cat# HY-N2117 |
| Hinokiflavone | MedChemExpress | Cat# HY-N2360 |
| eIF4A3-IN-1 | MedChemExpress | Cat# HY-101513 |
| NMDI14 | MedChemExpress | Cat# HY-111374 |
| Human recombinant YBX1 protein | Abcam | Cat# ab187443 |
| Cell counting kit (CCK-8) | Yeasen Biotech | Cat# 40203ES60 |

| | | |
|---|---|---|
| Annexin V FITC/PI apoptosis Kit | Multi Sciences | Cat# 70-APCC101-30 |
| Endotoxin-free plasmid purification kit | Tiangen | Cat# DP117 |
| PAGE-GEL silver staining kit | Solarbio | Cat# G7210 |
| FastPure® Cell/Tissue DNA isolation kit | Vazyme | Cat# DC112-01 |
| circRNA qRT-PCR kit | Geneseed | Cat# GS0201 |
| Fluorescent in situ hybridization kit | Ribobio | Cat# C10910 |
| FFPE RNA Kit | Omega Bio | Cat# R6954-02 |
| RNA-binding protein immunoprecipitation kit | Millipore | Cat# 17-701 |
| BeyoGold™ His-tag purification resin kit | Beyotime | Cat# P2218 |
| Pierce™ Streptavidin Magnetic Beads | Invitrogen | Cat# 88817 |
| BCA protein assay kit | Invitrogen | Cat# M34152 |
| Rhodamine phalloidin F-actin stain kit | Invitrogen | Cat# R415 |
| PARIS™ kit for nuclear and cytoplasmic RNA isolation | Invitrogen | Cat# AM1921 |
| Pierce™ Magnetic RNA-Protein pull-down kit | Invitrogen | Cat# 20164 |
| Dual-Luciferase reporter assay system kit | Promgea | Cat# E1910 |
| RiboMAX™ RNA production systems kit | Promega | Cat# P1280 |
| Competent cells: DH5α | Weidi Bio | N/A |
| Competent cells: BL21 | Weidi Bio | N/A |
| Plasmid: pLO5-ciR | Geneseed | Cat# GS0107 |
| Plasmid: pLC5-ciR (GFP) | Geneseed | Cat# GS0108 |
| Plasmid: pLVX-Puro | Youbio | Cat# VT1465 |
| Plasmid: lentiCRISPRv2 | TsingKe | N/A |
| Plasmid: pET-28a(+) | Youbio | Cat# VT1207 |
| Plasmid: pLO5-ciR-circASH2 | This paper | N/A |
| Plasmid: pLO5-ciR-circASH2-HRmut (1-14, 1+4+7+9) | This paper | N/A |
| Plasmid: pLO5-ciR-circASH2-YBX1mut (61-64, 80-84, 99-104. 526-530) | This paper | N/A |
| Plasmid: pLO5-ciR-circASH2-Random1,2 | This paper | N/A |
| Plasmid: pLO5-ciR-circPABPC1 | This paper | N/A |
| Plasmid: pLC5-ciR (GFP)-circASH2 | This paper | N/A |
| Plasmid: pLVX-Puro-TPM4 | This paper | N/A |
| Plasmid: pLVX-Puro-YBX1-FL-3xFlag | This paper | N/A |
| Plasmid: pLVX-Puro-YBX1-ΔAPD-3xFlag | This paper | N/A |
| Plasmid: pLVX-Puro-YBX1-ΔCSD-3xFlag | This paper | N/A |
| Plasmid: pLVX-Puro-YBX1-ΔCTD-3xFlag | This paper | N/A |
| Plasmid: pLVX-Puro-YBX1-FL-EGFP | This paper | N/A |
| Plasmid: pLVX-Puro-YBX1-ΔAPD-EGFP | This paper | N/A |
| Plasmid: pLVX-Puro-YBX1-ΔCTD-EGFP | This paper | N/A |
| Plasmid: lentiCRISPRv2-YBX1 | This paper | N/A |
| Plasmid: lentiCRISPRv2-TPM4 | This paper | N/A |
| Plasmid: lentiCRISPRv2-UPF1 | This paper | N/A |
| Plasmid: pET-28a(+)-YBX1-FL-EGFP | This paper | N/A |
| Plasmid: pET-28a(+)-YBX1-ΔAPD-EGFP | This paper | N/A |
| Plasmid: pET-28a(+)-YBX1-ΔCTD-EGFP | This paper | N/A |

| | | |
|---|---|---|
| Plasmid: pET-28a(+)-YBX1-ΔAPD+ΔCTD-EGFP | This paper | N/A |

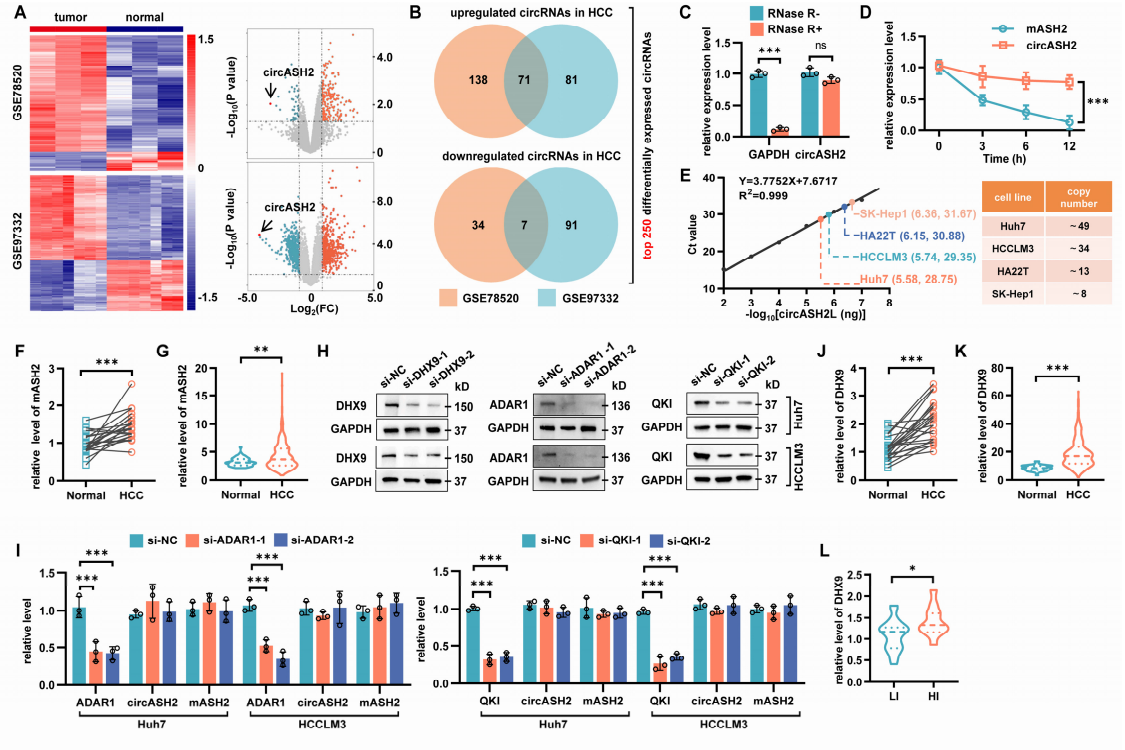


**Fig. S1. The microarray analysis identified circASH2 as a metastasis-suppressive role and regulated by DHX9 in HCC.**

**A.** A Heatmap (left) and a volcano plot (right) of differentially expressed circRNAs (|$\log_2$(fold-change)|≥ 1, $P$< 0.05) between normal tissues and HCC tissues in GSE78520 and GSE97332. circASH2 was denoted by black arrow.

**B.** A Venn Diagram showing differentially expressed circRNAs within GSE78520 and GSE97332.

**C.** RT-qPCR analysis of circASH2 after RNase R treatment in Huh7 cells. GAPDH mRNA was a negative control (mean ± SD, ***$P$ < 0.001, n.s., not significant, two-way ANOVA test).

**D.** The relative RNA levels were examined by RT-qPCR after treatment with actinomycin D at the indicated time points in Huh7 cells (mean ± SD, ***$P$ < 0.001, unpaired Student's t test).

**E.** Quantification of circASH2 copy numbers in 4 HCC cell lines. The Ct values and the amount of purified dsDNA fragments corresponding to circASH2 amplicon were plotted to generate a standard curve by RT-qPCR (left). $R^2$ represents Spearman's correlation coefficient and the $P$ value was calculated by Spearman's correlation test. The inset (right) presents the copy numbers of circASH2 in different HCC cells.

**F and G.** RT-qPCR analysis of mASH2 in 22-paired matched HCC and non-tumor tissues (F, cohort 1, mean ± SD, ***$P$ < 0.001, paired Student's t test), and TCGA HCC cohort (G, mean ± SD, **$P$ < 0.01, unpaired Student's t test).

**H.** HCC cells with DHX9 (left), ADAR1 (middle), QKI (right) knockdown were analyzed by immunoblotting with the indicated antibodies in Huh7 cells. GAPDH was used as an internal reference.

**I.** The expression levels of circASH2, mASH2, and ADAR1 or QKI were detected by RT-qPCR after treated with indicated siRNAs in Huh7 and HCCLM3 cells (mean ± SD, ***$P$ < 0.001, one-way ANOVA test).

**J, K and L.** The expression of DHX9 in 22-paired matched HCC and non-tumor tissues (J, cohort 1, ***$P$ < 0.001, paired Student's t test), TCGA HCC cohort (K, ***$P$ < 0.001, unpaired Student's t test) and 32 HI/LI HCC tissues (L, cohort 2, *$P$ < 0.05, unpaired Student's t test).

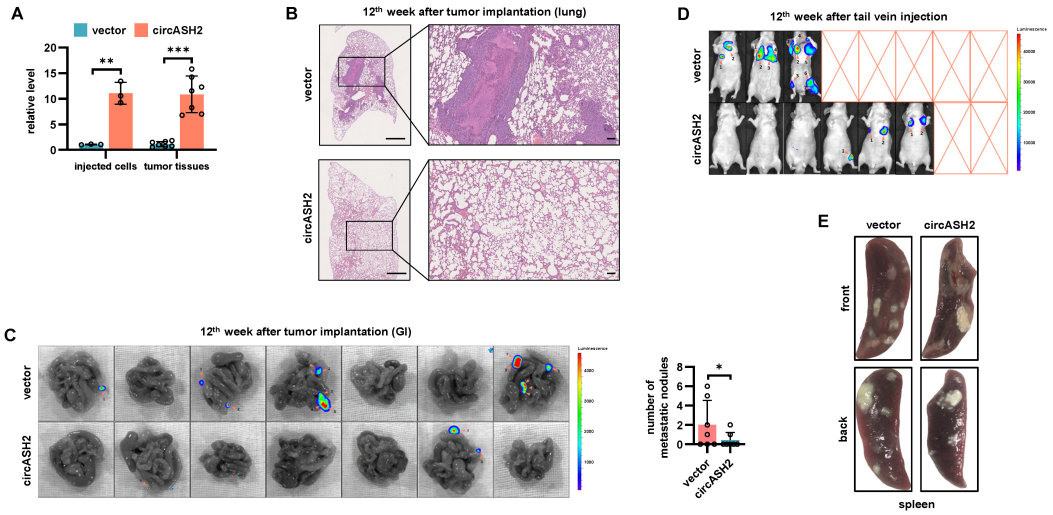


**Fig. S2. circASH2 suppresses HCC metastasis *in vivo.***

**A.** Confirmation of circASH2 overexpression in the injected cells and in situ tumors by RT-qPCR (***P* < 0.01. ****P* < 0.001, unpaired Student's *t* test). GAPDH was used as an internal reference.

**B.** Typical HE staining images (lung) of HA22T tumors at the 12th week after tumor implantation. Left: scale bar, 1 mm. Right: scale bar, 100 μm.

**C.** Left: IVIS images showing gastrointestinal (GI) metastasis in mice scarified at the 12th week (metastasis are marked with orange arrows, n=7). Right: GI metastasis are quantified (mean ±SD, **P* < 0.05, unpaired Student's t test).

**D.** IVIS images of HA22T tumors at the 12th week after rapid tail vein injection (metastasis are marked with orange arrows, n=8).

**E.** Typical spleen images of HA22T tumors in mice scarified at the 12th week.

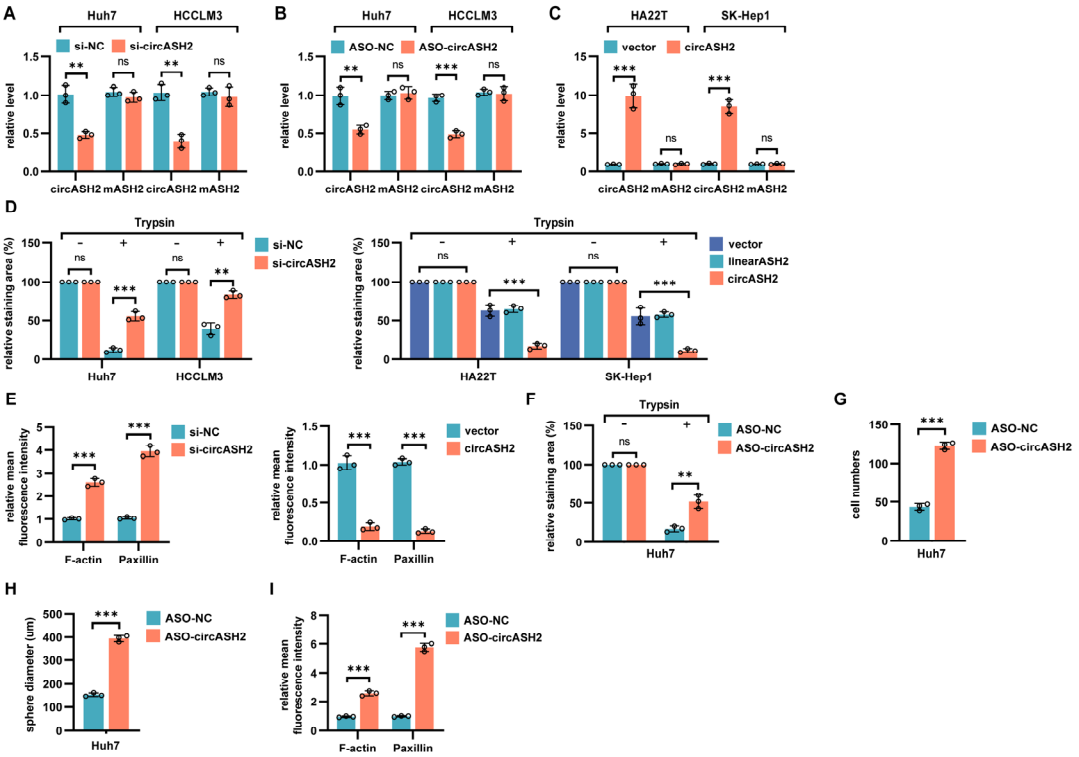


**Fig. S3 circASH2 impairs the cytoskeleton assembly in HCC.**
**A, B and C.** Confirmation of circASH2 knockdown (A and B) or overexpression (C) in HCC cells by RT-qPCR (***P* < 0.01. ****P* < 0.001, n.s., not significant, unpaired Student's *t* test). GAPDH was used as an internal reference.
**D and F.** Quantitative analysis on the photos of cells without (−) or with (+) trypsinization after crystal violet staining by staining area (means ± SD, ***P* < 0.01, ****P* < 0.001, n.s., not significant, unpaired Student's *t* test or one-way ANOVA test).
**E and I.** Quantitative analysis on the fluorescence photos by mean fluorescence intensity (means ± SD, ****P* < 0.001, unpaired Student's *t* test).
**G.** Quantitative analysis on the cell numbers per field of Transwell assays (means ± SD, ****P* < 0.001, unpaired Student's *t* test).
**H.** *In vitro* 3D invasion assays, the diameter of the sphere was measured and analyzed (****P* < 0.001, unpaired Student's t-test).

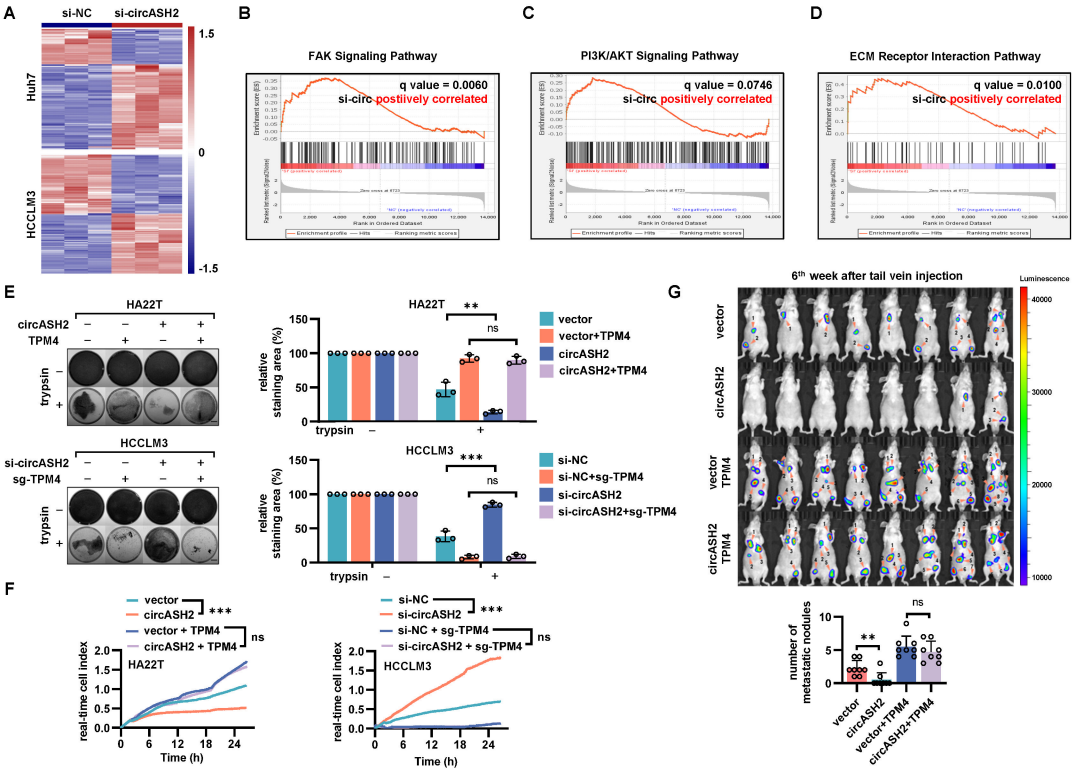


**Fig. S4 TPM4 is repressed by circASH2 and functionally relevant.**
**A.** A Heat Map showing the differentially expressed genes in HCC cells after circASH2 knock-down.
**B, C and D.** Gene set enrichment analysis (GSEA) showed FAK signaling pathway (B), PI3K/AKT signaling pathway (C), and ECM receptor interaction pathway were activated after circASH2 knock-down.
**E and F.** Ectopic expression of TPM4 rescued circASH2 induced phenotypes in trypsin digestion assays (E, $^{**}P < 0.01$, n.s., not significant, one-way ANOVA test) and dynamic metastasis assays (F, $^{***}P < 0.001$, n.s., not significant, two-way ANOVA test), while vice versa. Scale bar, 1 cm.
**G.** Up: IVIS images of HA22T tumors at the 6$^{th}$ week after rapid tail vein injection (metastasis are marked with orange arrows, n=8). Down: tumor foci are quantified (mean ± SD, $^{**}P < 0.01$, n.s., not significant, one-way ANOVA test).

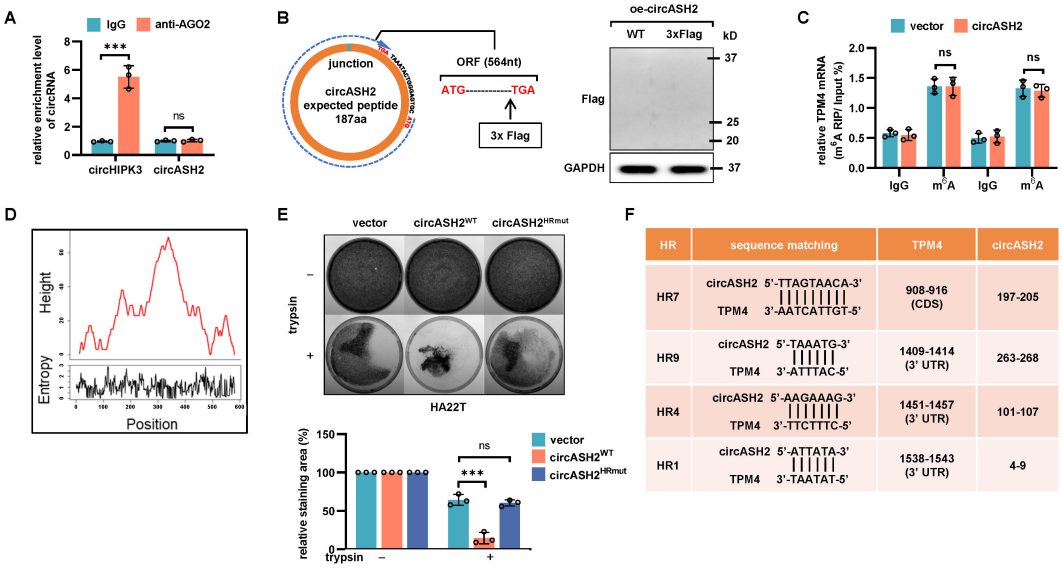


**Fig. S5 circASH2 promotes mRNA decay by physically connecting TPM4 transcripts.**
**A.** AGO2 RIP assays showed circASH2 cannot enriched by AGO2, while circHIPK3 (a well-known circRNA functions as miRNA sponge) was used as a positive control (***$P < 0.001$, and n.s., not significant, unpaired Student's *t* test).).
**B.** Left: ORF-Flag (cross junction-site) fusion construct was transfected into HA22T cells. The length of expected peptide encoded by circASH2 is 187aa (about 20-25 kd). Right: 187aa-Flag fusion protein was detected by immunoblot analysis. GAPDH was used as an internal reference.
**C.** The m6A level of TPM4 mRNA in HA22T cells with circASH2 overexpression was detected by m6A RIP experiment (n.s., not significant, unpaired Student's t-test).
**D.** A Mountain plot showing the MFE structure (upper) and the entropy (lower) for each position in circASH2.
**E.** Trypsin digestion assay on indicated HA22T cells. Cells without (−) or with (+) trypsinization were fix-stained with crystal violet and photographed (***$P < 0.001$, n.s., not significant, one-way ANOVA test). Scale bars, 1 cm.
**F.** A diagram showing TPM4 mRNA-circASH2 matching sequences (analysis by BLAST) and positions.

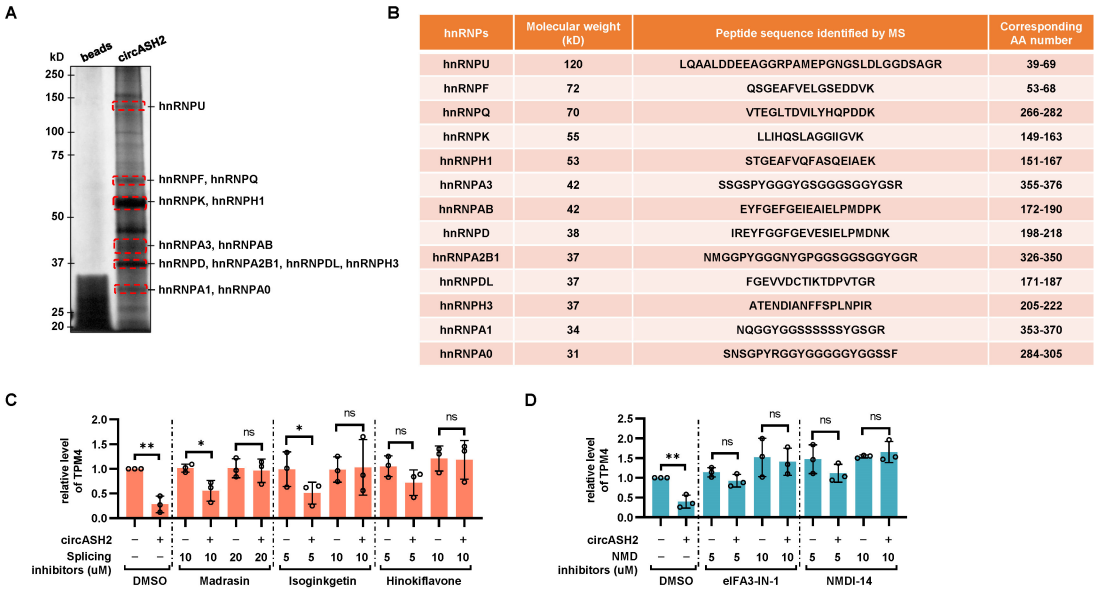


| hnRNPs | Molecular weight (kD) | Peptide sequence identified by MS | Corresponding AA number |
|---|---|---|---|
| hnRNPU | 120 | LQAALDDEEAGGRPAMEPGNGSLDLGGDSAGR | 39-69 |
| hnRNPF | 72 | QSGEAFVELGSEDDVK | 53-68 |
| hnRNPQ | 70 | VTEGLTDVILYHQPDDK | 266-282 |
| hnRNPK | 55 | LLIHQSLAGGIIGVK | 149-163 |
| hnRNPH1 | 53 | STGEAFVQFASQEIAEK | 151-167 |
| hnRNPA3 | 42 | SSGSPYGGGYGSGGGSGGYGSR | 355-376 |
| hnRNPAB | 42 | EYFGEFGEIEAIELPMDPK | 172-190 |
| hnRNPD | 38 | IREYFGGFGEVESIELPMDNK | 198-218 |
| hnRNPA2B1 | 37 | NMGGPYGGGNYGPGGSGGSGGYGGR | 326-350 |
| hnRNPDL | 37 | FGEVVDCTIKTDPVTGR | 171-187 |
| hnRNPH3 | 37 | ATENDIANFFSPLNPIR | 205-222 |
| hnRNPA1 | 34 | NQGGYGGSSSSSSYGSGR | 353-370 |
| hnRNPA0 | 31 | SNSGPYRGGYGGGGGYGGSSF | 284-305 |

**Fig. S6 circASH2/hnRNPs complex accelerates mRNA degradation via nonsense-mediated decay.**

**A.** Potential circASH2-binding proteins (purified by circRNA pulldown) were separated by SDS-PAGE and visualized by silver staining. hnRNP bands were highlighted with red box.

**B.** A diagram showing the characteristic peptides in corresponding bands detected by mass spectrometry.

**C.** HA22T cells overexpressing circASH2 or control vector were treated with DMSO, Madrasin (10-20 μM), Isoginkgetin (5-10 μM), or Hinokiflavone (5-10 μM) for 48 hours. The endogenous TPM4 protein bands were quantified and standardized by GAPDH (means ± SD, **P* < 0.05, ***P* < 0.01, n.s., not significant, one-way ANOVA test).

**D.** HA22T cells overexpressing circASH2 or control vector were treated with DMSO, eIF4A3-IN-1 (5-10 μM), NMDI-14 (5-10 μM) for 48 hours. The endogenous TPM4 protein bands were quantified and standardized by GAPDH (means ± SD, ***P* < 0.01, n.s., not significant, one-way ANOVA test).

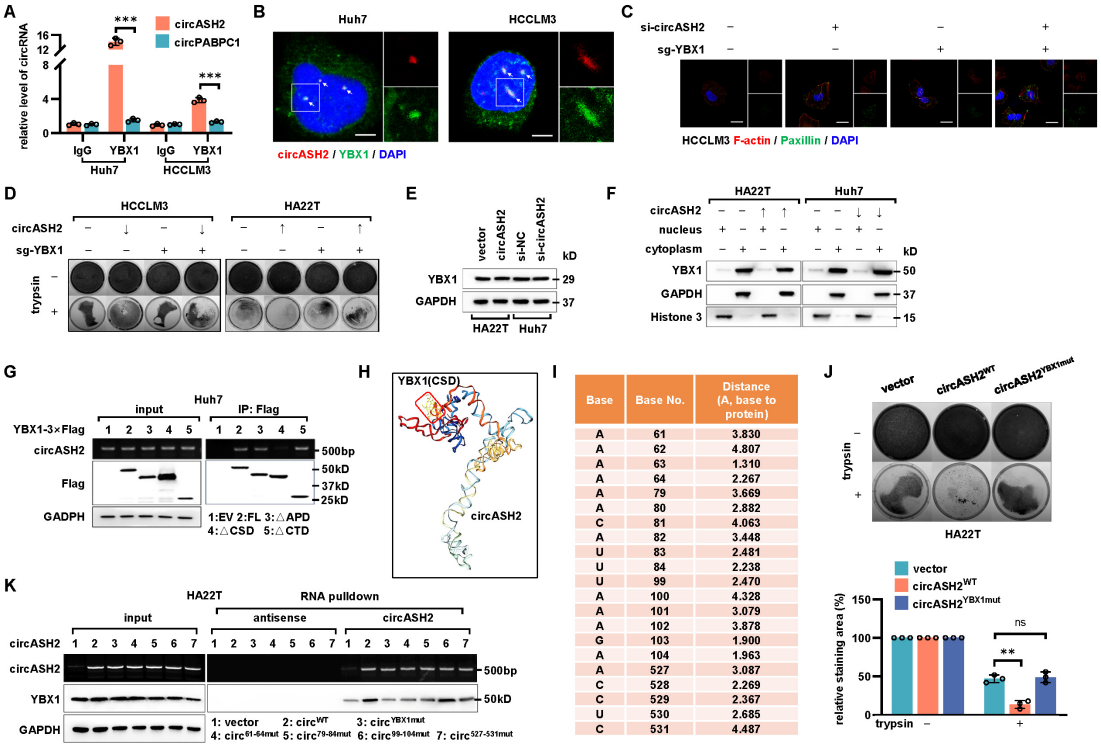


**Fig. S7 circASH2/hnRNPs-induced TPM4 mRNA degradation is YBX1-dependent.**

**A.** RT-qPCR was used to detect the endogenous circASH2 immunoprecipitated with YBX1, while circPABPC1 acted as a negative control (***$P < 0.001$, unpaired Student's t-test).

**B.** circASH2 FISH (red) and anti-YBX1 immunofluorescence (green) staining showing colocalization of these two molecules (arrowheads) in Huh7 and HCCLM3 cells. Nuclei were labeled with DAPI (blue). Scale bars, 10 μm.

**C.** Cytoskeleton formation of indicated HCCLM3 cells was shown by phalloidin staining of F-actin (red) and immunofluorescence of paxillin (green), while DAPI (blue) was used to stain the nucleus. Scale bar, 10 μm.

**D.** Trypsin digestion assay on indicated HCC cells. Cells without (−) or with (+) trypsinization were fix-stained with crystal violet and photographed. Scale bars, 1 cm.

**E.** The expression level of YBX1 was detected by immunoblot after circASH2 overexpression (HA22T) or knockdown (Huh7) in HCC cells.

**F.** The nuclear-cytoplasmic distribution of YBX1 was determined by immunoblot after circASH2 overexpression (HA22T) or knockdown (Huh7) in HCC cells.

**G.** Huh7 cells were transduced with $YBX1^{FL}$-3×Flag, $YBX1^{\Delta APD}$-3×Flag, $YBX1^{\Delta CSD}$-3×Flag and $YBX1^{\Delta CTD}$-3×Flag, respectively. RT-qPCR was used to detect the circASH2 enriched by anti-Flag immunoprecipitation.

**H.** Simulated interaction between circASH2 and YBX1 (CSD, denoted by red box) generated by HDOCK.

**I.** A diagram showing the circASH2 bases predicted to interact with YBX1.

**J.** Trypsin digestion assay on indicated HA22T cells. Cells without (−) or with (+) trypsinization were fix-stained with crystal violet and photographed (**$P < 0.01$, n.s., not significant, one-way ANOVA test). Scale bars, 1 cm.

**K.** HA22T cells were transduced with $circASH2^{WT}$, $circASH2^{YBX1mut}$, $circASH2^{61\text{-}64mut}$, $circASH2^{79\text{-}84mut}$, $circASH2^{99\text{-}104mut}$, and $circASH2^{527\text{-}531mut}$, respectively. Immunoblots analysis was used to detect the endogenous YBX1 enriched by circASH2-pulldown

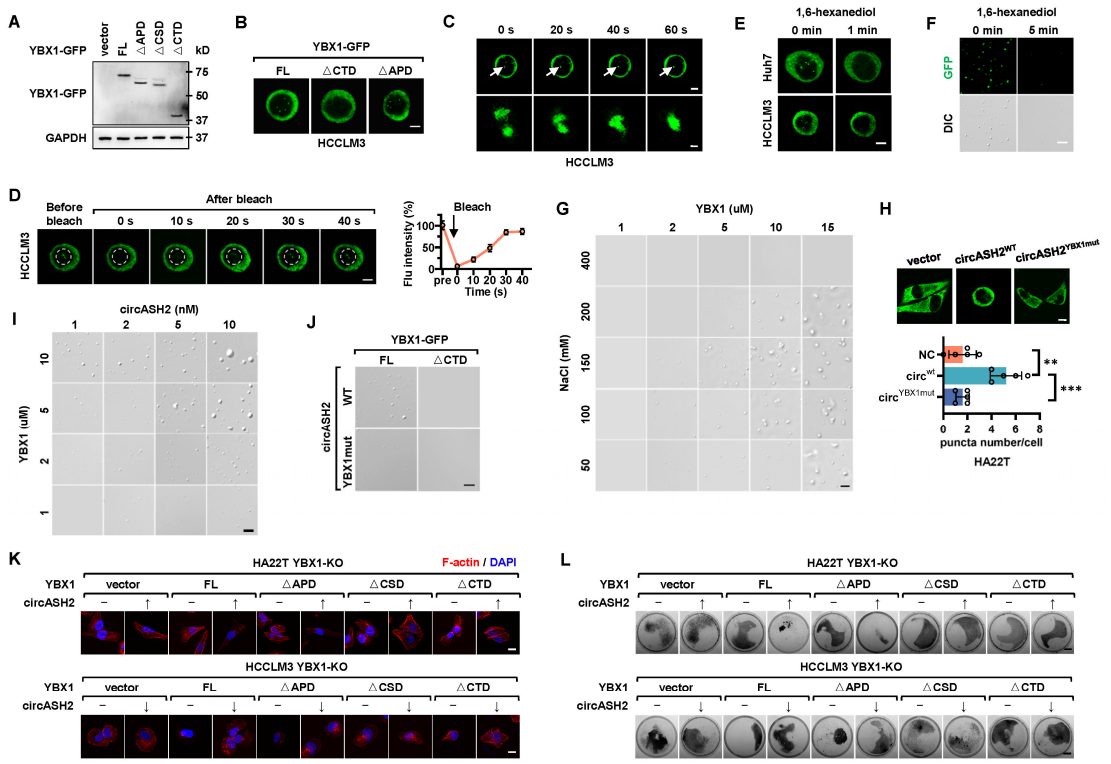


**Fig. S8 Intranuclear YBX1 undergoes LLPS enhanced by circASH2, and is indispensable for circASH2 signals.**

**A.** YBX1$^{FL}$-GFP and a series of YBX1-GFP truncation mutations were generated and determined by immunoblots analysis. GAPDH was used as an internal reference.

**B.** HCCLM3 cells transfected with YBX1$^{FL}$-GFP, YBX1$^{\triangle CTD}$-GFP, or YBX1$^{\triangle APD}$-GFP were analyzed by confocal microscopy. Representative pictures were shown. Scale bar, 10 μm.

**C.** Time-series fluorescence microscopy analysis of YBX1-GFP puncta in HCCLM3 cells. Bottom row shows zoom-in view of two fusing puncta. Scale bar, 10 μm (top) and 2 μm (bottom).

**D.** Left: Representative micrographs of YBX1-GFP puncta before and after photobleaching in HCCLM3 cells. Scale bar, 10 μm. Right: Quantification of fluorescence intensity recovery in the bleached region of YBX1 puncta.

**E and F.** The effect of 5% 1,6-hexanediol on YBX1 droplets *in vivo* (E, scale bar, 10 μm) and *in vitro* (F, scale bar, 5 μm).

**G.** Representative images of phase separation behaviors of different concentrations of purified YBX1-GFP in different concentrations of NaCl (with 5% PEG8000). Scale bar, 5 μm.

**H.** Top: Representative images of YBX1-GFP in control and circASH2-overexpressed HA22T cells. Scale bar, 10 μm. Bottom: Quantification of YBX1-GFP puncta number in control and circASH2-overexpressed HA22T cells (mean ± SD, **P < 0.01, one-way ANOVA test).

**I.** *In vitro* phase separation assay showing that circASH2 promotes YBX1 LLPS in a dose-dependent manner. Scale bar, 5 μm.

**J.** *In vitro* phase separation assay showing that circASH2$^{WT}$ facilitates YBX1$^{WT}$-GFP, instead of YBX1$^{\triangle CTD}$-GFP, phase separation, whereas circASH2$^{YBX1mut}$ loses the function. Scale bar, 5 μm.

**K and L.** YBX1-KO HCC cells (HCCLM3 and HA22T) were reconstituted with YBX1$^{FL}$, YBX1$^{\triangle APD}$, YBX1$^{\triangle CSD}$, and YBX1$^{\triangle CTD}$, respectively. Cytoskeleton formation (K) in indicated cells was shown by phalloidin staining of F-actin (red), while DAPI was used to stain the nucleus. Scale bar, 10 μm. Meanwhile, representative images of trypsin digestion assay (L) on indicated cells were shown. Scale bars, 1 cm.

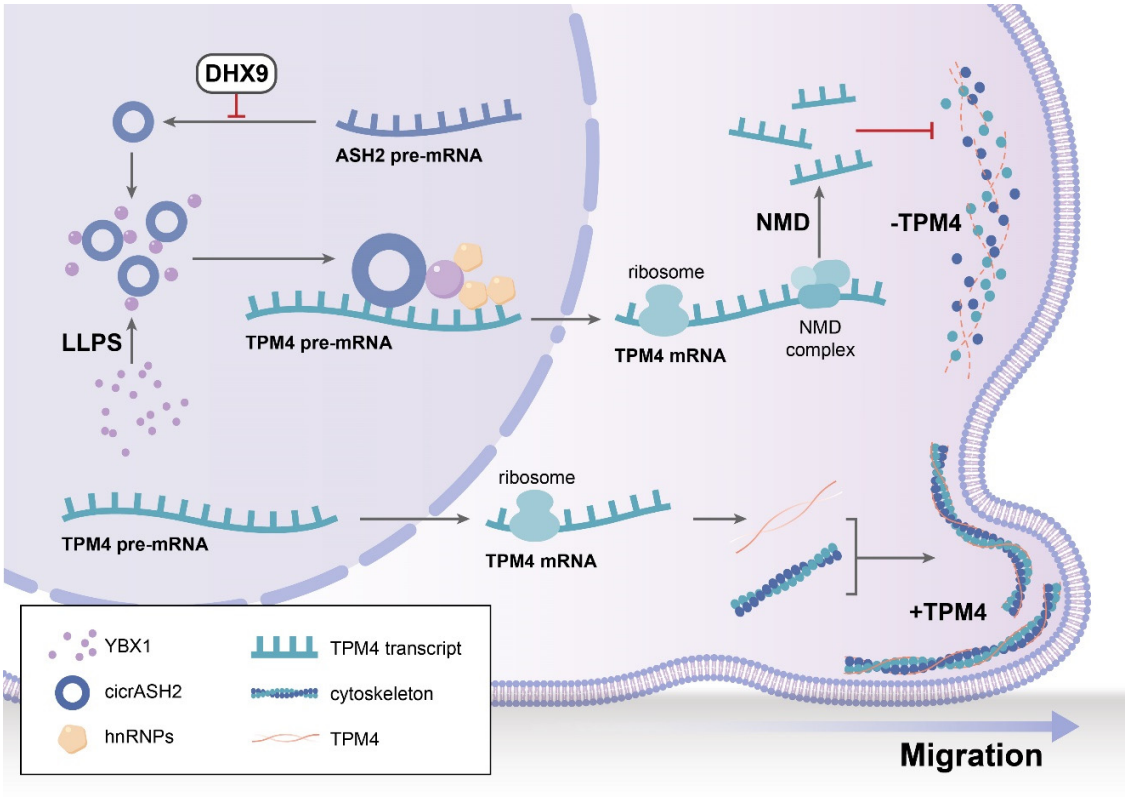


**Fig. S9 Schematic diagram.** circASH2 s negatively regulated by DHX9 and connects TPM4 transcripts with the YBX1/hnRNPs complex, thereby facilitating NMD of the former. Decreased TPM4 results in cytoskeletal instability, which in turn inhibits HCC metastasis. Furthermore, circASH2 promotes YBX1 LLPS and augments YBX1-mediated TPM4 transcripts' decay.

**Table S1. Clinical characteristics of 5 HI and 5 LI HCC patients.**

| Number | Gender | Age (years) | Pathology | Tumor size (cm) | Postsurgical metastasis |
|---|---|---|---|---|---|
| HI-1 | M | 80 | moderately differentiated HCC, MVI:0 | 1.7×1.4 | Y |
| HI-2 | M | 65 | moderately-poorly differentiated HCC, MVI:0 | 2.8×2.5 | Y |
| HI-3 | M | 61 | well-moderately differentiated HCC, MVI:1 | 2.0×1.5 | Y |
| HI-4 | M | 65 | well-moderately differentiated HCC, MVI:0 | 2.0×1.8 | Y |
| HI-5 | M | 64 | moderately differentiated HCC, MVI:0 | 2.7×2.7 | Y |
| LI-1 | M | 63 | well-moderately differentiated HCC, MVI:0 | 8.0×6.0 | N |
| LI-2 | F | 65 | well-moderately differentiated HCC, MVI:0 | 8.5×6.5 | N |
| LI-3 | M | 59 | moderately differentiated HCC, MVI:1 | 7.0×4.5 | N |
| LI-4 | M | 62 | moderately differentiated HCC, MVI:0 | 3.5×3.0 | N |
| LI-5 | M | 68 | moderately-poorly differentiated HCC, MVI:1 | 4.3×3.0 | N |

**Table S2. Clinicopathological analyses of 91 primary HCC patients with different expression levels of circASH2 (cohort 3).**

| Variables | | circASH2 | | *P* value |
|---|---|---|---|---|
| | | High | Low | |
| Age, years | ≤60 | 26 | 27 | 0.999 |
| | >60 | 19 | 19 | |
| Gender | Female | 11 | 7 | 0.303 |
| | Male | 34 | 39 | |
| HBV | No | 10 | 5 | 0.168 |
| | Yes | 35 | 41 | |
| Cirrhosis | No | 21 | 21 | 0.999 |
| | Yes | 24 | 25 | |
| AFP, ng/mL | ≤400 | 27 | 27 | 0.900 |
| | >400 | 18 | 19 | |
| Tumor size, cm | ≤5 | 30 | 21 | 0.058 |
| | >5 | 15 | 25 | |
| Recurrence | No | 22 | 15 | 0.138 |
| | Yes | 23 | 31 | |

**Table S3. Mass spectrometry identified the potential circASH2-binding proteins (unused valve＞10).**

| Protein | Unused value | Protein | Unused value |
|---|---|---|---|
| YBX1 | 89.66 | PCCB | 21.04 |
| PYC | 77.36 | HNRNPA3 | 19.67 |
| HNRNPD | 58.95 | HNRPQ | 19.34 |
| HNRNPA1 | 51.56 | ANXA2 | 18.43 |
| RFA1 | 50.50 | HNRNPAB | 18.14 |
| PARP1 | 49.38 | RS4X | 17.74 |
| SSBP | 45.04 | EFTU | 17.19 |
| MCCB | 44.88 | HNRNPH | 16.00 |
| TBB5 | 44.53 | HNRNPU | 15.41 |
| TBA1B | 41.90 | PCBP2 | 14.42 |
| PURB | 41.02 | DAZP1 | 14.39 |
| RFA2 | 35.93 | RS3A | 14.07 |
| PURA | 30.66 | RS18 | 13.77 |
| HNRNPA2 | 30.35 | TCP4 | 12.99 |
| PUR9 | 28.75 | HNRNPL | 12.91 |
| HMCES | 28.21 | RS6 | 12.07 |
| TREX1 | 26.36 | MCCA | 12.02 |
| ACACA | 25.25 | UGDH | 11.70 |
| HLTF | 23.72 | ALDH2 | 11.66 |
| MGME1 | 23.15 | MSI2H | 11.62 |
| HNRNPK | 22.36 | KPYM | 10.10 |
| RBMS1 | 22.22 | RLA0L | 10.01 |

**Table S4. Structural disorder analysis of YBX1 amino acid sequence.**

| AA No. | AA | PrD-like score | Disorder score |
|---|---|---|---|
| 1 | M | 0.0089 | 0.9813 |
| 2 | S | 0.0075 | 0.9792 |
| 3 | S | 0.0059 | 0.9785 |
| 4 | E | 0.0038 | 0.9784 |
| 5 | A | 0.0039 | 0.9777 |
| 6 | E | 0.0039 | 0.977 |
| 7 | T | 0.0066 | 0.9748 |
| 8 | Q | 0.0107 | 0.9744 |
| 9 | Q | 0.0116 | 0.9731 |
| 10 | P | 0.0111 | 0.9738 |
| 11 | P | 0.0104 | 0.9741 |
| 12 | A | 0.0094 | 0.9743 |
| 13 | A | 0.0086 | 0.9753 |
| 14 | P | 0.0079 | 0.9752 |
| 15 | P | 0.007 | 0.9736 |
| 16 | A | 0.0059 | 0.971 |
| 17 | A | 0.0049 | 0.9677 |
| 18 | P | 0.0041 | 0.9632 |
| 19 | A | 0.0031 | 0.9558 |
| 20 | L | 0.0021 | 0.9454 |
| 21 | S | 0.002 | 0.9208 |
| 22 | A | 0.0017 | 0.8889 |
| 23 | A | 0.0015 | 0.8446 |
| 24 | D | 0.0013 | 0.789 |
| 25 | T | 0.0015 | 0.7159 |
| 26 | K | 0.0019 | 0.6402 |
| 27 | P | 0.0038 | 0.573 |
| 28 | G | 0.0054 | 0.504 |
| 29 | T | 0.0064 | 0.4483 |
| 30 | T | 0.008 | 0.4014 |
| 31 | G | 0.0106 | 0.3651 |
| 32 | S | 0.0123 | 0.3699 |
| 33 | G | 0.0135 | 0.3742 |
| 34 | A | 0.0142 | 0.3844 |
| 35 | G | 0.015 | 0.3973 |
| 36 | S | 0.0153 | 0.4194 |
| 37 | G | 0.0153 | 0.4414 |
| 38 | G | 0.0148 | 0.4638 |
| 39 | P | 0.0138 | 0.4883 |
| 40 | G | 0.0124 | 0.5063 |
| 41 | G | 0.0103 | 0.5256 |
| 42 | L | 0.0069 | 0.5418 |
| 43 | T | 0.0061 | 0.5315 |
| 44 | S | 0.0057 | 0.5305 |
| 45 | A | 0.0051 | 0.5349 |

| | | | |
|---|---|---|---|
| 46 | A | 0.0046 | 0.5382 |
| 47 | P | 0.0041 | 0.5351 |
| 48 | A | 0.0035 | 0.5276 |
| 49 | G | 0.003 | 0.5211 |
| 50 | G | 0.002 | 0.5217 |
| 51 | D | 0.0005 | 0.5225 |
| 52 | K | 0.0001 | 0.519 |
| 53 | K | 0 | 0.5226 |
| 54 | V | 0 | 0.5355 |
| 55 | I | 0 | 0.5515 |
| 56 | A | 0.0001 | 0.5687 |
| 57 | T | 0 | 0.5828 |
| 58 | K | 0 | 0.6045 |
| 59 | V | 0 | 0.6275 |
| 60 | L | 0 | 0.6397 |
| 61 | G | 0.0001 | 0.639 |
| 62 | T | 0.0001 | 0.6416 |
| 63 | V | 0.0001 | 0.6458 |
| 64 | K | 0.0001 | 0.6467 |
| 65 | W | 0.0002 | 0.6512 |
| 66 | F | 0.0012 | 0.6424 |
| 67 | N | 0.0029 | 0.6254 |
| 68 | V | 0.0032 | 0.6099 |
| 69 | R | 0.0043 | 0.5868 |
| 70 | N | 0.0062 | 0.5612 |
| 71 | G | 0.0064 | 0.5393 |
| 72 | Y | 0.0063 | 0.5243 |
| 73 | G | 0.0058 | 0.5027 |
| 74 | F | 0.0047 | 0.4841 |
| 75 | I | 0.0042 | 0.4654 |
| 76 | N | 0.0045 | 0.4449 |
| 77 | R | 0.0036 | 0.437 |
| 78 | N | 0.0033 | 0.4345 |
| 79 | D | 0.0011 | 0.4326 |
| 80 | T | 0.0005 | 0.4348 |
| 81 | K | 0.0001 | 0.4406 |
| 82 | E | 0 | 0.4464 |
| 83 | D | 0 | 0.4523 |
| 84 | V | 0 | 0.4616 |
| 85 | F | 0.0001 | 0.4657 |
| 86 | V | 0.0001 | 0.4656 |
| 87 | H | 0.0003 | 0.4639 |
| 88 | Q | 0.0005 | 0.4549 |
| 89 | T | 0.0004 | 0.45 |
| 90 | A | 0.0003 | 0.4485 |
| 91 | I | 0.0002 | 0.4431 |
| 92 | K | 0.0002 | 0.4315 |
| 93 | K | 0.0005 | 0.4237 |

| | | | |
|---|---|---|---|
| 94 | N | 0.0017 | 0.4164 |
| 95 | N | 0.0019 | 0.4086 |
| 96 | P | 0.0014 | 0.4046 |
| 97 | R | 0.0007 | 0.4052 |
| 98 | K | 0.0004 | 0.4096 |
| 99 | Y | 0.0003 | 0.4271 |
| 100 | L | 0.0002 | 0.4316 |
| 101 | R | 0.0002 | 0.4339 |
| 102 | S | 0.0002 | 0.4386 |
| 103 | V | 0.0001 | 0.4532 |
| 104 | G | 0.0001 | 0.4637 |
| 105 | D | 0.0001 | 0.4709 |
| 106 | G | 0.0001 | 0.4785 |
| 107 | E | 0 | 0.4836 |
| 108 | T | 0 | 0.4944 |
| 109 | V | 0 | 0.5057 |
| 110 | E | 0 | 0.5079 |
| 111 | F | 0 | 0.5197 |
| 112 | D | 0 | 0.5186 |
| 113 | V | 0 | 0.5229 |
| 114 | V | 0 | 0.5131 |
| 115 | E | 0 | 0.4994 |
| 116 | G | 0.0001 | 0.492 |
| 117 | E | 0.0001 | 0.4834 |
| 118 | K | 0.0003 | 0.4811 |
| 119 | G | 0.0013 | 0.4765 |
| 120 | A | 0.0019 | 0.4715 |
| 121 | E | 0.0026 | 0.4717 |
| 122 | A | 0.0088 | 0.4772 |
| 123 | A | 0.0159 | 0.4992 |
| 124 | N | 0.0241 | 0.5117 |
| 125 | V | 0.0258 | 0.5337 |
| 126 | T | 0.0314 | 0.5526 |
| 127 | G | 0.0401 | 0.5635 |
| 128 | P | 0.0459 | 0.5931 |
| 129 | G | 0.0508 | 0.6263 |
| 130 | G | 0.0539 | 0.6672 |
| 131 | V | 0.0557 | 0.712 |
| 132 | P | 0.062 | 0.7421 |
| 133 | V | 0.0673 | 0.7634 |
| 134 | Q | 0.0833 | 0.778 |
| 135 | G | 0.0872 | 0.8091 |
| 136 | S | 0.0894 | 0.8369 |
| 137 | K | 0.0911 | 0.8632 |
| 138 | Y | 0.1015 | 0.8976 |
| 139 | A | 0.1077 | 0.9123 |
| 140 | A | 0.1149 | 0.9197 |
| 141 | D | 0.1233 | 0.9206 |

| | | | |
|---|---|---|---|
| 142 | R | 0.1544 | 0.9167 |
| 143 | N | 0.2109 | 0.9184 |
| 144 | H | 0.2244 | 0.9222 |
| 145 | Y | 0.2409 | 0.9214 |
| 146 | R | 0.2507 | 0.906 |
| 147 | R | 0.269 | 0.8875 |
| 148 | Y | 0.3022 | 0.877 |
| 149 | P | 0.3224 | 0.8391 |
| 150 | R | 0.3399 | 0.8076 |
| 151 | R | 0.3719 | 0.7778 |
| 152 | R | 0.4299 | 0.77 |
| 153 | G | 0.5351 | 0.767 |
| 154 | P | 0.6053 | 0.762 |
| 155 | P | 0.6664 | 0.7578 |
| 156 | R | 0.7197 | 0.7564 |
| 157 | N | 0.8161 | 0.7766 |
| 158 | Y | 0.8394 | 0.798 |
| 159 | Q | 0.8535 | 0.7791 |
| 160 | Q | 0.8566 | 0.776 |
| 161 | N | 0.8552 | 0.7692 |
| 162 | Y | 0.8453 | 0.7525 |
| 163 | Q | 0.8289 | 0.6968 |
| 164 | N | 0.7666 | 0.6322 |
| 165 | S | 0.5093 | 0.5523 |
| 166 | E | 0.2008 | 0.464 |
| 167 | S | 0.1647 | 0.4119 |
| 168 | G | 0.1213 | 0.3482 |
| 169 | E | 0.0563 | 0.2753 |
| 170 | K | 0.0488 | 0.2485 |
| 171 | N | 0.0477 | 0.2237 |
| 172 | E | 0.0408 | 0.2119 |
| 173 | G | 0.0409 | 0.2207 |
| 174 | S | 0.0403 | 0.2467 |
| 175 | E | 0.0392 | 0.2716 |
| 176 | S | 0.0433 | 0.3212 |
| 177 | A | 0.0465 | 0.3695 |
| 178 | P | 0.0503 | 0.4126 |
| 179 | E | 0.0535 | 0.4752 |
| 180 | G | 0.083 | 0.5658 |
| 181 | Q | 0.1027 | 0.6374 |
| 182 | A | 0.1076 | 0.7 |
| 183 | Q | 0.1133 | 0.7688 |
| 184 | Q | 0.1136 | 0.8137 |
| 185 | R | 0.1091 | 0.8493 |
| 186 | R | 0.1071 | 0.8918 |
| 187 | P | 0.1069 | 0.927 |
| 188 | Y | 0.1062 | 0.9563 |
| 189 | R | 0.104 | 0.9693 |

| | | | |
|---|---|---|---|
| 190 | R | 0.1036 | 0.9778 |
| 191 | R | 0.1048 | 0.983 |
| 192 | R | 0.1081 | 0.9884 |
| 193 | F | 0.1146 | 0.9922 |
| 194 | P | 0.1266 | 0.9929 |
| 195 | P | 0.1369 | 0.9936 |
| 196 | Y | 0.1458 | 0.9943 |
| 197 | Y | 0.151 | 0.9937 |
| 198 | M | 0.1536 | 0.992 |
| 199 | R | 0.1549 | 0.9883 |
| 200 | R | 0.1586 | 0.9845 |
| 201 | P | 0.1661 | 0.9793 |
| 202 | Y | 0.1724 | 0.9723 |
| 203 | G | 0.1759 | 0.9576 |
| 204 | R | 0.1776 | 0.9352 |
| 205 | R | 0.1819 | 0.9183 |
| 206 | P | 0.1905 | 0.8923 |
| 207 | Q | 0.1979 | 0.8704 |
| 208 | Y | 0.1984 | 0.8661 |
| 209 | S | 0.1971 | 0.8471 |
| 210 | N | 0.195 | 0.8313 |
| 211 | P | 0.1823 | 0.8254 |
| 212 | P | 0.1677 | 0.8252 |
| 213 | V | 0.1508 | 0.8261 |
| 214 | Q | 0.1453 | 0.8257 |
| 215 | G | 0.1231 | 0.8247 |
| 216 | E | 0.0896 | 0.828 |
| 217 | V | 0.0861 | 0.8486 |
| 218 | M | 0.0859 | 0.8433 |
| 219 | E | 0.0847 | 0.82 |
| 220 | G | 0.0913 | 0.8291 |
| 221 | A | 0.0954 | 0.8359 |
| 222 | D | 0.1003 | 0.8253 |
| 223 | N | 0.1192 | 0.8192 |
| 224 | Q | 0.1233 | 0.8116 |
| 225 | G | 0.1227 | 0.8118 |
| 226 | A | 0.1207 | 0.8079 |
| 227 | G | 0.1192 | 0.8025 |
| 228 | E | 0.1162 | 0.804 |
| 229 | Q | 0.1207 | 0.8322 |
| 230 | G | 0.1203 | 0.8653 |
| 231 | R | 0.1187 | 0.8971 |
| 232 | P | 0.1188 | 0.9245 |
| 233 | V | 0.1185 | 0.9488 |
| 234 | R | 0.1217 | 0.9601 |
| 235 | Q | 0.1281 | 0.9755 |
| 236 | N | 0.1286 | 0.9849 |
| 237 | M | 0.1237 | 0.9911 |

| | | | |
|---|---|---|---|
| 238 | Y | 0.1165 | 0.9939 |
| 239 | R | 0.1044 | 0.9946 |
| 240 | G | 0.0978 | 0.9951 |
| 241 | Y | 0.0878 | 0.9953 |
| 242 | R | 0.0711 | 0.994 |
| 243 | P | 0.0619 | 0.9924 |
| 244 | R | 0.0514 | 0.99 |
| 245 | F | 0.0456 | 0.9883 |
| 246 | R | 0.0425 | 0.9775 |
| 247 | R | 0.0411 | 0.9556 |
| 248 | G | 0.0408 | 0.9161 |
| 249 | P | 0.0397 | 0.8615 |
| 250 | P | 0.0383 | 0.7984 |
| 251 | R | 0.0365 | 0.691 |
| 252 | Q | 0.0359 | 0.5535 |
| 253 | R | 0.0315 | 0.4436 |
| 254 | Q | 0.0293 | 0.3469 |
| 255 | P | 0.0198 | 0.25 |
| 256 | R | 0.0088 | 0.1658 |
| 257 | E | 0.0028 | 0.1362 |
| 258 | D | 0.0021 | 0.1269 |
| 259 | G | 0.0021 | 0.1151 |
| 260 | N | 0.0019 | 0.0944 |
| 261 | E | 0.0005 | 0.08 |
| 262 | E | 0.0003 | 0.0802 |
| 263 | D | 0.0006 | 0.0934 |
| 264 | K | 0.0015 | 0.1096 |
| 265 | E | 0.0058 | 0.1275 |
| 266 | N | 0.0424 | 0.1677 |
| 267 | Q | 0.0512 | 0.2245 |
| 268 | G | 0.0531 | 0.2899 |
| 269 | D | 0.054 | 0.3328 |
| 270 | E | 0.0594 | 0.3729 |
| 271 | T | 0.1071 | 0.5025 |
| 272 | Q | 0.182 | 0.6218 |
| 273 | G | 0.2018 | 0.6985 |
| 274 | Q | 0.2148 | 0.7386 |
| 275 | Q | 0.2174 | 0.8148 |
| 276 | P | 0.2146 | 0.8657 |
| 277 | P | 0.2111 | 0.9123 |
| 278 | Q | 0.2069 | 0.9416 |
| 279 | R | 0.1885 | 0.9593 |
| 280 | R | 0.1786 | 0.973 |
| 281 | Y | 0.1734 | 0.9826 |
| 282 | R | 0.1644 | 0.9834 |
| 283 | R | 0.1598 | 0.9842 |
| 284 | N | 0.1579 | 0.9857 |
| 285 | F | 0.1463 | 0.9881 |

| | | | |
|---|---|---|---|
| 286 | N | 0.1399 | 0.9824 |
| 287 | Y | 0.1123 | 0.976 |
| 288 | R | 0.067 | 0.9543 |
| 289 | R | 0.042 | 0.921 |
| 290 | R | 0.0282 | 0.8782 |
| 291 | R | 0.0206 | 0.8166 |
| 292 | P | 0.0165 | 0.7336 |
| 293 | E | 0.0116 | 0.6584 |
| 294 | N | 0.0114 | 0.5847 |
| 295 | P | 0.009 | 0.5376 |
| 296 | K | 0.0062 | 0.5016 |
| 297 | P | 0.0058 | 0.5637 |
| 298 | Q | 0.0052 | 0.6134 |
| 299 | D | 0.0023 | 0.6981 |
| 300 | G | 0.0016 | 0.7733 |
| 301 | K | 0.0003 | 0.8161 |
| 302 | E | 0.0001 | 0.8556 |
| 303 | T | 0.0001 | 0.8949 |
| 304 | K | 0.0001 | 0.9278 |
| 305 | A | 0.0001 | 0.9559 |
| 306 | A | 0.0001 | 0.9663 |
| 307 | D | 0.0002 | 0.967 |
| 308 | P | 0.0003 | 0.9676 |
| 309 | P | 0.0004 | 0.9658 |
| 310 | A | 0.0004 | 0.9646 |
| 311 | E | 0.0004 | 0.9575 |
| 312 | N | 0.001 | 0.9556 |
| 313 | S | 0.001 | 0.9574 |
| 314 | S | 0.001 | 0.9534 |
| 315 | A | 0.0008 | 0.9473 |
| 316 | P | 0.0006 | 0.926 |
| 317 | E | 0.0003 | 0.9092 |
| 318 | A | 0.0004 | 0.9142 |
| 319 | E | 0.0006 | 0.9041 |
| 320 | Q | 0.0019 | 0.9055 |
| 321 | G | 0.0022 | 0.9049 |
| 322 | G | 0.0022 | 0.9139 |
| 323 | A | 0.002 | 0.9157 |
| 324 | E | 0.0018 | 0.9005 |

**Reference**


1. Shi L*, et al.* (2017) Circular RNA expression is suppressed by androgen receptor (AR)-regulated adenosine deaminase that acts on RNA (ADAR1) in human hepatocellular carcinoma. *Cell Death Dis* 8(11):e3171.
2. Sanjana NE, Shalem O, & Zhang F (2014) Improved vectors and genome-wide libraries for CRISPR screening. *Nat Methods* 11(8):783-784.
3. Hofacker IL & Stadler PF (2006) Memory efficient folding algorithms for circular RNA secondary structures. *Bioinformatics* 22(10):1172-1176.
4. Zuker M (2003) Mfold web server for nucleic acid folding and hybridization prediction. *Nucleic acids research* 31(13):3406-3415.
5. Popenda M*, et al.* (2012) Automated 3D structure composition for large RNAs. *Nucleic acids research* 40(14):e112.
6. Zhu P*, et al.* (2019) IL-13 secreted by ILC2s promotes the self-renewal of intestinal stem cells through circular RNA circPan3. *Nat Immunol* 20(2):183-194.
7. Yan Y, Zhang D, Zhou P, Li B, & Huang SY (2017) HDOCK: a web server for protein-protein and protein-DNA/RNA docking based on a hybrid strategy. *Nucleic acids research* 45(W1):W365-W373.